

Electronic structures and magnetic properties of rare-earth-atom-doped BNNTs

Juan Ren^{1,3,†}, Ning-Chao Zhang², Peng Wang¹, Chao Ning¹, Hong Zhang³, Xiao-Juan Peng⁴

¹School of Science, Xi'an Technological University, Xi'an 710032, China

²College of Electronics and Information Engineering, Xi'an Technological University, Xi'an 710032, China

³College of Physical Science and Technology, Sichuan University, Chengdu 610065, China

⁴Institute of Fluid Physics, China Academy of Engineering Physics, Mianyang 621900, China

Corresponding author. E-mail: †renjuan@xatu.edu.cn

Received May 30, 2015; accepted July 25, 2015

Stable geometries, electronic structures, and magnetic properties of (8,0) and (4,4) single-walled BN nanotubes (BNNTs) doped with rare-earth (RE) atoms are investigated using the first-principles pseudopotential plane wave method with density functional theory (DFT). The results show that these RE atoms can be effectively doped in BNNTs with favorable energies. Because of the curvature effect, the values of binding energy for RE-atom-doped (4,4) BNNTs are larger than those of the same atoms on (8,0) BNNTs. Electron transfer between RE-5*d*, 6*s*, and B-2*p*, N-2*p* orbitals was also observed. Furthermore, electronic structures and magnetic properties of BNNTs can be modified by such doping. The results show that the adsorption of Ce, Pm, Sm, and Eu atoms can induce magnetization, while no magnetism is observed when BNNTs are doped with La. These results are useful for spintronics applications and for developing magnetic nanostructures.

Keywords density functional theory, RE atoms, single-walled BN nanotubes, doping

PACS numbers 81.07.De, 68.43.-h, 73.22.-f

1 Introduction

Since its discovery by Iijima, carbon nanotubes (CNTs) have attracted a great deal of attention because of their interesting optical, electronic, superconducting, and magnetic properties [1–3]. Boron nitride nanotube (BNNT) is an important lightweight nanotube. Unlike CNTs, BNNTs are semiconductors with a large band gap of 4.0–5.8 eV, and are almost independent of tube chirality and morphology [4]. Moreover, they possess excellent mechanic properties, high thermal stability, high thermal conductivity, and outstanding chemical inertness, and hence, they have been extensively investigated in recent years [5–9].

Functionalization is an efficient approach to tune the physical properties of materials through various methods, such as chemical bonding, doping, defect, and adsorption. Many studies have investigated the adsorption of transition-metal (TM) atoms on the surface of single-walled carbon nanotubes (SWCNTs) or SWCNT bundles. SWCNTs have applications in many fields [10–16].

Zhou *et al.* [17] have shown that when the concentration of defects is increased in SWCNTs, their band gaps decrease. It has been recently shown that the electronic structures and magnetic properties of the ZnO monolayer can be modified by TM doping [18]. The functionalized BNNTs have many applications. The adsorption of transition metals on the (8,0) boron nitride nanotube has been investigated, and it has been shown that the adsorption of TM atoms can change the electronic and magnetic properties of pure BNNTs by introducing impurity states [19]. Wang *et al.* [20] investigated the electronic structure and optical property of 3*d* TM-doped (5,5) BNNTs. They showed that doping systems are ideal candidates for spintronics or diluted magnetic semiconductor materials. C-doped BNNTs have been successfully synthesized and it has been predicted that their electronic structure can be tuned [21–25]. In addition, doped systems of BNNTs have been shown to possess promising potential for gas-storage media. The adsorption of H₂, NO, N₂O, O₂, CO, CO₂, C₂H₄, C₂H₂, H₂O, NH₃, and other small molecules onto BNNTs and doped BNNTs has been studied with the help of density func-

tional theory [26–30].

However, to our knowledge, the adsorption of rare-earth (RE) atoms on BNNTs has been rarely studied. In this work, we performed a comprehensive first-principles study on RE atom adsorption on single-walled (8,0) and (4,4) BNNTs. The rest of the paper is organized as follows. The computational method details are given in Section 2. In Section 3, we discuss RE atom adsorption on BNNTs, and also discuss their adsorption energies, bond lengths, bond angles, Mulliken charge, and magnetic moments. The electronic structure, spin charge density, and density of state (DOS) of the functional systems are analyzed in detail for each case. The results demonstrate that BNNTs can be magnetized by doping with certain RE atoms.

2 Method

All calculations were carried out by using the DMol³ program [31, 32] based on the density functional theory. The generalized gradient approximation (GGA) with the Perdew, Burke, and Ernzerhof (PBE) functional was employed to describe the exchange and correlation terms. DFT calculations with GGA treat the nonlocality of exchange-correlation better than local density approximation (LDA) [33, 34]. The DFT semicore pseudopotential (DSPP) was performed to determine the relativistic effect, which replaces core electrons as a single effective potential [35]; a double numerical plus d-function (DND) was selected. Structural optimizations were obtained without any symmetry constraints by using a convergence tolerance of energy of 1.0×10^{-5} Ha, a maximum force of 0.002 Ha/Å, and a maximum displacement of 0.005 Å. The orbital cutoff was set to be global with a value of 4.5 Å, and smearing was 0.005 Ha.

The binding energy was calculated by the following

formula:

$$E_b = E(\text{BNNT}) + E(\text{RE}) - E(\text{RE_BNNT})$$

where $E(\text{RE_BNNT})$ is the spin-polarized total energy of the optimized configuration of RE-doped BNNTs, $E(\text{RE})$ is the energy of an isolated RE atom, and $E(\text{BNNT})$ is the energy of pure BNNTs.

3 Results discussion

First, pure armchair (8,0) and zigzag (4,4) BNNTs were fully optimized and their electronic band structures were calculated by considering spin polarization. Before investigating the adsorption of RE atoms on the BNNTs, pure armchair (8,0) and zigzag (4,4) BNNTs were obtained, and their spin-polarized electronic band structures were determined (Fig. 1). The symmetry between majority spin and minority spin states was investigated by band structure analysis, and it was found that pure (8,0) and (4,4) BNNTs have no magnetism. To conduct a suitable comparison of adatom adsorption on BNNTs, it is important to determine the conditions required for energetically favorable adsorption of RE atoms. For this, we considered the following five possible different initial sites to adsorb RE atoms: (i) top of the B atom (B site); (ii) top of the N atom (N site); (iii) the hexagon center (H site); (iv) armchair direction (BA site); and (v) zigzag direction (BZ site) [Fig. 1(a)]. After full structural optimization, all RE atoms are found to locate on the top of the H site, regardless of the initial location of the RE atoms. The tube structures changed slightly on RE-atom doping.

Based on the optimization structures, we calculated the average distance of the RE atom to the six nearest B and N atoms to determine the binding energy, magnetic moment, and Mulliken charge. As shown in Table 1, Sm

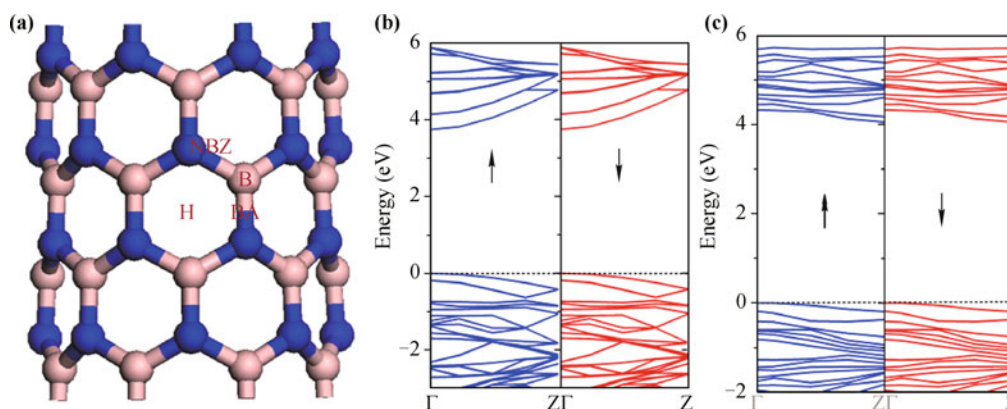


Fig. 1 (a) five different adsorption sites of BNNTs, including (i) the on-top of the B atom (B site); (ii) the on-top of the N atom (N site); (iii) the centre of the hexagon (H site); (iv) the armchair direction (BA site); (v) the zigzag direction (BZ site), the electronic band structure of (b) pure (8,0) BNNT and (c) pure (4,4) BNNT. The Fermi level is set to zero.

Table 1 Summary of results for RE metal atoms adsorbed on the (8,0) and (4,4) BN nanotubes. The average distance (\AA) of adatom to six nearest B and N atoms, binding energies (eV), the magnetic moments of the RE impurities μ_{RE} (μ_{B}), RE-doped BNNT system magnetic moment $\mu_{\text{RE-BNNT}}$ (μ_{B}) per supercell and Mulliken charge (a.u.) of RE atoms are listed, respectively.

System	$D_{\text{AE-N}}$	$D_{\text{AE-B}}$	E_{b}	μ_{RE}	$\mu_{\text{RE-BNNT}}$	Charge
La-(8,0)BNNT	2.810	2.841	1.087	0	0	0.248
Ce-(8,0)BNNT	2.773	2.810	2.155	2.163	2.080	0.427
Pm-(8,0)BNNT	2.895	2.965	1.494	5.968	6.173	0.193
Sm-(8,0)BNNT	2.906	2.981	6.608	7.284	7.723	0.292
Eu-(8,0)BNNT	2.944	3.022	0.495	8.270	8.837	0.286
La-(4,4)BNNT	2.729	2.734	5.663	0	0	0.327
Ce-(4,4)BNNT	2.809	2.820	6.657	-1.906	-1.961	0.503
Pm-(4,4)BNNT	2.869	2.925	5.846	6.341	7.017	0.105
Sm-(4,4)BNNT	2.855	2.919	10.437	-7.019	-7.338	0.292
Eu-(4,4)BNNT	2.913	2.974	4.852	8.319	8.887	0.253

is the most favorable dopant for both (8,0) and (4,4) BNNTs with binding energies of 6.608 and 10.437 eV, respectively, which are the largest values. In contrast, the adsorption energy of Eu is the smallest for both (8,0) and (4,4) BNNTs. However, positive binding energies of all configurations indicate that the chemical adsorption process is exothermic. Thus, it can be concluded that the values of binding energies are suitable enough to dope both (8,0) and (4,4) BNNTs. After adsorption on (8,0) BNNTs, however, the binding energy of an individual RE atom becomes lower than that observed with (4,4) BNNTs. This trend can be explained by the curvature effect [36]. The average B-RE (RE = La, Ce, Pm, Sm, and Eu) bond lengths range from 2.773 to 2.944 \AA , while the N-RE bond lengths range from 2.734 to 3.022 \AA . An important aspect of RE-doped BNNTs is their magnetic behavior. The magnetic moments are also listed in Table 1. These results show that no magnetism is observed when La atom is adsorbed on the BNNTs. This phenomenon can also be observed for La adsorption on SWCNTs [36]. In this study, the local magnetic moments for Ce, Pm, Sm, and Eu are 2.163, 5.968, 7.284, and 8.270 μ_{B} , respectively, for adsorption on (8,0) BNNTs, and are -1.960, 6.341, -7.019, and 8.319 μ_{B} , respectively, for adsorption on (4,4) BNNTs. The nearest-neighbor B and N atoms of RE atoms make only a small contribution to the total magnetic moments. Analysis of spin charge density distribution of Ce, Pm, Sm, and Eu shows that the magnetism is mainly contributed by the RE atoms (in Fig. 3). This indicates that most of the spin density is localized around the RE adatom. The magnetic moments of adatoms are predominantly contributed by the polarized $5d6s$ electrons and the localized $4f$ electrons. Mulliken charge analysis of the single RE atom adsorbed on BNNTs shows that metal atoms donate electrons to the neighboring B and N atoms of the BNNTs (Table 1). Upon metal doping, most of the $6s$ electrons of La

transfer to neighboring B- $2p$ and N- $2p$ orbitals, whereas $4f$ electrons of Ce, Pm, Sm, and Eu remain in the orbital. This phenomenon may explain why the magnetic moment of Ce, Pm, Sm, and Eu is maintained but that of La becomes zero. Based on these results, we surmise that the magnetic moments of the RE-adsorption BNNT systems should originate from the doped RE impurities, because the ground state of pure BNNTs is nonmagnetic.

Figure 2 shows that comparison of spin-polarized band structures of doped-BNNTs with that of pure BNNTs. For pure (8,0) BNNTs, both the valence band maximum (VBM) and the conduction band minimum (CBM) are located at the Γ symmetry point with a gap (Γ - Γ) of 3.788 eV and an indirect gap (Γ - Z) of 4.062 eV for the (4,4) BNNTs. We observed that the majority (spin-up) and minority (spin-down) band structures of La-adsorption BNNTs are identical, with zero magnetic moment for La atom. In La-doped (8,0) BNNTs, a small energy gap (0.864 eV) is present just near the Fermi energy level. A comparison of the bands of La-doped (4,4) BNNTs with those of bare (4,4) BNNTs shows that the valence band of La lies near the Fermi level and the energy gap decreases to 0.573 eV. In the case of Ce-doped (8,0) BNNT, the majority spin state is semimetallic with an energy gap of 0.058 eV and the minority spin state is semiconducting with an energy gap of 0.919 eV. However, the situation is different for Ce adsorption on (4,4) BNNTs, where both the spin-up and spin-down states are semiconducting with energy gaps of 0.718 and 0.233 eV, respectively. The Pm-doped (8,0) BNNT is a semiconductor with a direct band gap of 0.121 eV for the spin-up channel and of 3.392 eV for the spin-down channel. In the case of Pm-doped (4,4) BNNT, the spin-up and spin-down band gaps are 0.804 and 4.097 eV, respectively. The Sm-doped (8,0) BNNT is a semiconductor with a direct band gap of 0.528 eV for the spin-up channel and that of 3.615 eV for the spin-down channel.

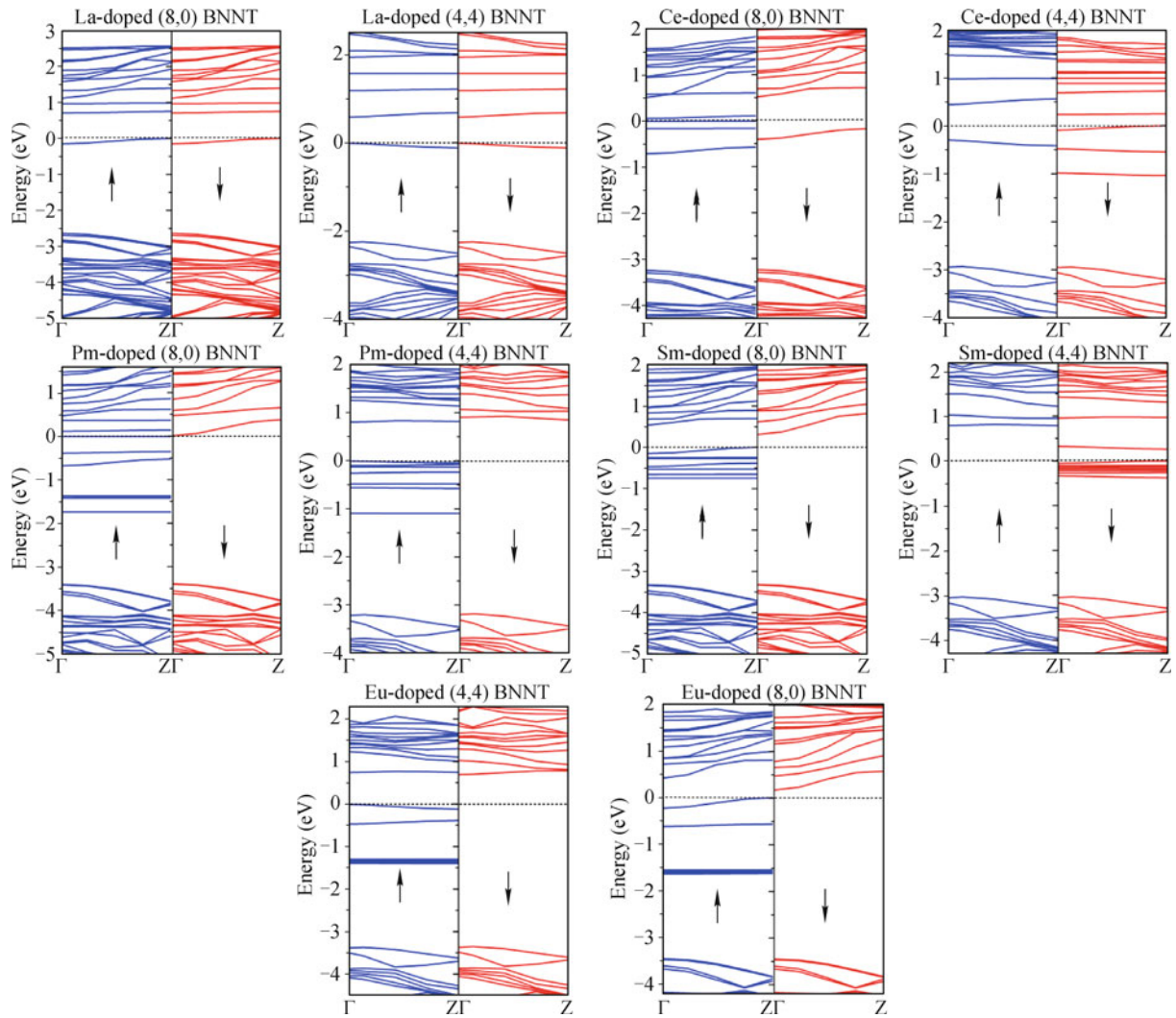


Fig. 2 Band structures of RE (RE=La, Ce, Pm, Sm, and Eu) doped (8,0) and (4,4) BNNTs, respectively. The horizontal dotted line represents the Fermi energy level.

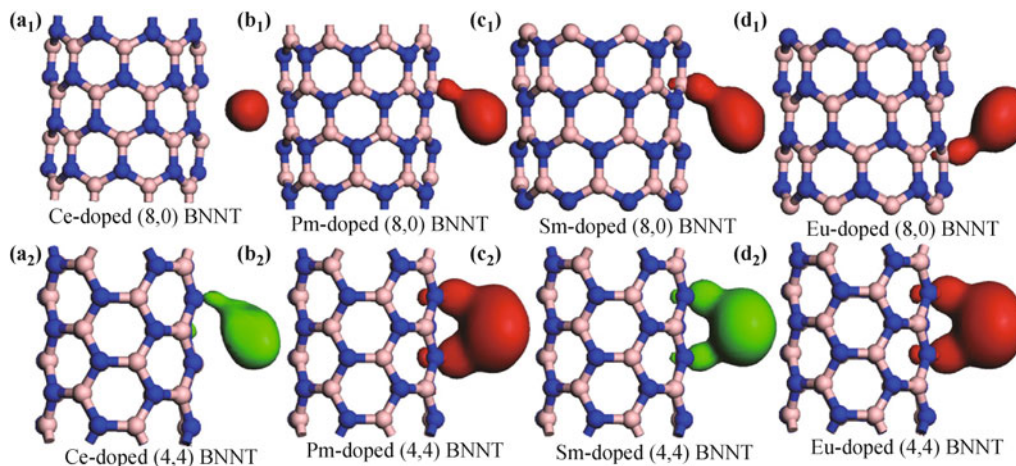


Fig. 3 The spin charge density distribution of RE (RE=Ce, Pm, Sm, and Eu) doped (a_1 – d_1) BNNTs (isovalues=0.05 $e/\text{\AA}$) and (a_2 – d_2) BNNTs (isovalues=0.03 $e/\text{\AA}$), respectively. The red and green colors represent positive (spin-up) and negative (spin-down) values, respectively.

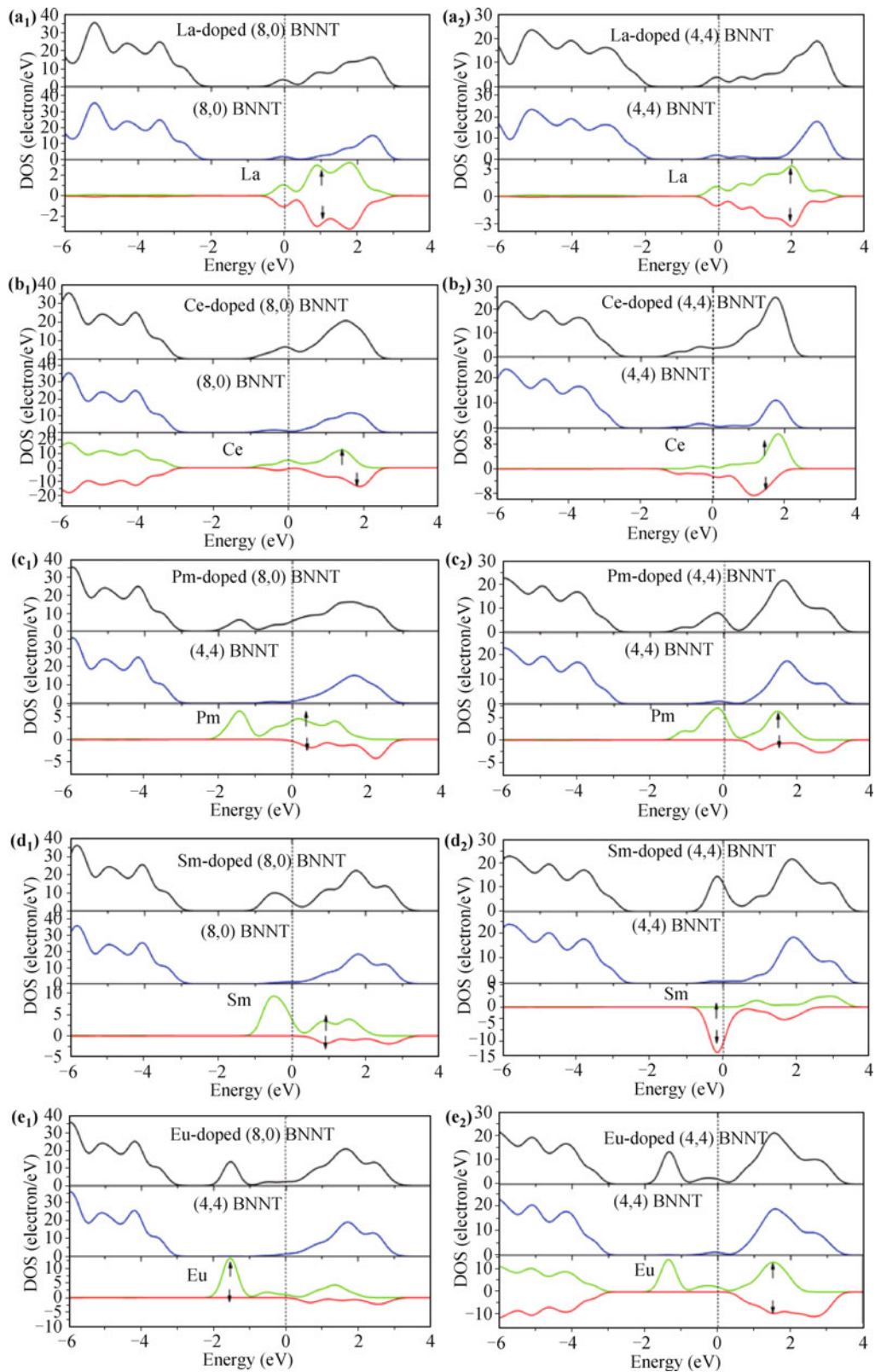


Fig. 4 The local density of states (LDOS) of RE (RE= La, Ce, Pm, Sm, and Eu) atoms doped on (8,0) and (4,4) BNNTs, colored lines represent up-spin and down-spin, respectively. The Fermi level is set zero energy and indicated by the vertical dashed lines.

In the case of Sm-doped (4,4) BNNT, the spin-up and spin-down band gaps are 3.861 and 0.262 eV, respectively. In the Eu-doped (8,0) BNNT, both the majority and minority spin states are semiconducting with band gaps of 0.640 and 3.611 eV, respectively. In the case of Eu-doped (4,4) BNNT, the spin-up and spin-down band gaps are 0.731 and 4.078 eV, respectively.

To further evaluate the electron distribution using the energy of the doped RE atoms and the spin-up and spin-down states, we present the local density of states (LDOS) of the RE atoms for all configurations (Fig. 4). The Fermi level is set to zero and is indicated by the vertical dashed lines. As shown in Figs. 4(a₁) and (a₂), for the La-doped (8,0) and (4,4) BNNTs, both the spin-up and spin-down DOSs of La are completely symmetrical, indicating the nonmagnetic state of the systems. It can also be seen that the Ce-, Pm-, Sm-, and Eu-doped BNNTs are magnetic, because there is a clear spin polarization between the DOSs of the two spin channels at/near the Fermi level. The analyzed LDOS results are entirely consistent with the calculated magnetic properties and band structures in the former. In order to understand the origin of magnetism, the projected DOSs of doped and pure BNNTs are also plotted in Fig. 4. Taking the Sm-doped (8,0) BNNTs as an example, we analyzed the magnetic moments, band structure, and DOS together in detail. The Sm-doped (8,0) BNNT is a semiconductor with an indirect band gap of 0.528 eV for the spin-up channel. A few bands above the Fermi level correspond to Sm's orbitals, as can be seen from the DOS in Fig. 4(d₁). The Sm-doped (8,0) BNNT is a semiconductor with a direct band gap of 3.615 eV for the spin-up state. In the spin-down channels, we can see that the bands above Fermi energy are very similar to those of spin-down channels. However, six nearly flat bands appear at 0–0.8 eV below the Fermi level for spin-up, and disappear for spin-down states. The total magnetic moment per supercell of Sm-doped (8,0) BNNTs is 7.723 μ_B , and the local magnetic moment of the Sm atom is 7.284 μ_B , while the sum of the neighboring B and N atoms' contribution is 0.439 μ_B . Similar analysis can be obtained for the doped BNNT systems.

4 Conclusions

This study presents a comprehensive investigation of the structures and electronic and magnetic properties of BNNTs doped with RE atoms (La, Ce, Pm, Sm, and Eu). The adsorption energies indicate that the doping is suitable, and the optimized structures show that RE atom adsorption leads to structural distortion around the

RE impurity compared to pure BNNTs. The electronic structure of the BNNTs is significantly changed after RE incorporation. Furthermore, the doping of BNNTs with Ce, Pm, Sm, and Eu atoms can induce magnetization. However, La-doped BNNTs show no magnetism. These results may help in understanding the effect of RE metal adsorption on BNNTs.

Acknowledgements This work was supported by the Research Fund for the Doctoral Program of Xi'an Technological University (Grant No. 204-000317).

References

1. S. Iijima, Helical microtubules of graphitic carbon, *Nature* 354(6348), 56 (1991)
2. R. H. Baughman, A. A. Zakhidov, and W. A. de Heer, Carbon nanotubes — the route toward applications, *Science* 297(5582), 787 (2002)
3. D. Tasis, N. Tagmatarchis, A. Bianco, and M. Prato, Chemistry of carbon nanotubes, *Chem. Rev.* 106(3), 1105 (2006)
4. V. Bougrov, M. E. Levinshtein, S. L. Rumyantsev, M. E. Levinshtein, S. L. Rumyantsev, and M. S. Shur, Properties of Advanced Semiconductor Materials: GaN, AlN, InN, BN, SiC, SiGe, New York: Wiley, 2001
5. D. Golberg, Y. Bando, C. C. Tang, and C. Y. Zhi, Boron nitride nanotubes, *Adv. Mater.* 19(18), 2413 (2007)
6. Z. Zhou and Y. F. Li, How different are BN nanotubes from carbon nanotubes? *J. Comput. Theor. Nanosci.* 6(2), 327 (2009)
7. C. Y. Zhi, Y. Bando, C. C. Tang, and D. Golberg, Engineering of electronic structure of boron-nitride nanotubes by covalent functionalization, *Phys. Rev. B* 74(15), 153413 (2006)
8. L. Lai, W. Song, J. Lu, Z. Gao, S. Nagase, M. Ni, W. N. Mei, J. Liu, D. Yu, and H. Ye, Structural and electronic properties of fluorinated boron nitride nanotubes, *J. Phys. Chem. B* 110(29), 14092 (2006)
9. J. Zhang, K. P. Loh, W. S. Yang, and P. Wu, Exohedral doping of single-walled boron nitride nanotube by atomic chemisorption, *Appl. Phys. Lett.* 87(24), 243105 (2005)
10. C. Jo, C. Kim, and Y. H. Lee, Electronic properties of K-doped single-wall carbon nanotube bundles, *Phys. Rev. B* 65(3), 035420 (2002)
11. J. Zhao, A. Buldum, J. Han, and J. P. Lu, First-principles study of Li-intercalated carbon nanotube ropes, *Phys. Rev. Lett.* 85(8), 1706 (2000)
12. J. W. Zheng, S. M. L. Nai, M. F. Ng, P. Wu, J. Wei, and M. Gupta, DFT study on nano structures of Sn/CNT complex for potential li-ion battery application, *J. Phys. Chem. C* 113(31), 14015 (2009)
13. E. Durgun, S. Dag, V. M. K. Bagci, O. Gülseren, T. Yildirim, and S. Ciraci, Systematic study of adsorption of single atoms

- on a carbon nanotube, *Phys. Rev. B* 67(20), 201401 (2003)
14. E. Durgun, S. Dag, S. Ciraci, and O. Gülseren, Energetics and electronic structures of individual atoms adsorbed on carbon nanotubes, *J. Phys. Chem. B* 108(2), 575 (2004)
 15. Y. L. Mao, X. H. Yan, and Y. Xiao, First-principles study of transition-metal-doped single-walled carbon nanotubes, *Nanotechnology* 16(12), 3092 (2005)
 16. A. Udomvech, T. Kerdcharoen, and T. Osotchan, First principles study of Li and Li⁺ adsorbed on carbon nanotube: Variation of tubule diameter and length, *Chem. Phys. Lett.* 406(1?3), 161 (2005)
 17. Q. X. Zhou, C. Y. Wang, Z. B. Fu, Y. J. Tang, and H. Zhang, Effects of various defects on the electronic properties of single-walled carbon nanotubes: A first principle study, *Front. Phys.* 9(2), 200 (2014)
 18. J. Ren, H. Zhang, and X. L. Cheng, Electronic and magnetic properties of all 3 *d* transition-metal-doped ZnO monolayers, *Int. J. Quantum Chem.* 113(19), 2243 (2013)
 19. X. Wu and X. C. Zeng, Adsorption of transition-metal atoms on boron nitride nanotube: A density-functional study, *J. Chem. Phys.* 125(4), 44711 (2006)
 20. S. F. Wang, Y. Zhang, J. M. Zhang, K. W. Xu, and V. Ji, Electronic structure and optical property of 3d transition metal doped (5,5) boron nitride nanotube, *Appl. Phys. A* 109(3), 601 (2012)
 21. R. J. Baierle, T. M. Schmidt, and A. Fazzio, Adsorption of CO and NO molecules on carbon doped boron nitride nanotubes, *Solid State Commun.* 142(1–2), 49 (2007)
 22. Y. F. Zhukovskii, S. Bellucci, S. Piskunov, L. Trinkler, and B. Berzina, Atomic and electronic structure of single-walled BN nanotubes containing N vacancies as well as C and O substitutes of N atoms, *Eur. Phys. J. B* 67(4), 519 (2009)
 23. C. S. Guo, W. J. Fan, and R. Q. Zhang, Spin polarization of the injected carriers in C-doped BN nanotubes, *Solid State Commun.* 137(5), 246 (2006)
 24. C. Y. Zhi, X. D. Bai, and E. G. Wang, Boron carbonitride nanotubes, *J. Nanosci. Nanotechnol.* 4(1–2), 35 (2004)
 25. C. Zhi, Y. Bando, C. Tang, and D. Golberg, Boron nitride nanotubes, *Mater. Sci. Eng. Rep.* 70(3–6), 92 (2010)
 26. H. Choi, Y. C. Park, Y. H. Kim, and Y. S. Lee, Ambient carbon dioxide capture by boron-rich boron nitride nanotube, *J. Am. Chem. Soc.* 133(7), 2084 (2011)
 27. Y. Xie, Y. P. Huo, and J. M. Zhang, First-principles study of CO and NO adsorption on transition metals doped (8,0) boron nitride nanotube, *Appl. Surf. Sci.* 258(17), 6391 (2012)
 28. X. M. Li, W. Q. Tian, X. R. Huang, C. C. Sun, and L. Jiang, Adsorption of hydrogen on novel Pt-doped BN nanotube: A density functional theory study, *J. Mol. Struct.* 901(1–3), 103 (2009)
 29. Q. Dong, X. M. Li, W. Q. Tian, X. R. Huang, and C. C. Sun, Theoretical studies on the adsorption of small molecules on Pt-doped BN nanotubes, *J. Mol. Struct.* 948(1–3), 83 (2010)
 30. M. T. Baei, A. R. Soltani, A. V. Moradi, and E. T. Lemeski, Adsorption properties of N₂O on (6,0), (7,0), and (8,0) zigzag single-walled boron nitride nanotubes: A computational study, *Comput. Theor. Chem.* 970(1–3), 30 (2011)
 31. J. P. Perdew, and Y. Wang, Accurate and simple analytic representation of the electron-gas correlation energy, *Phys. Rev. B* 45(23), 13244 (1992)
 32. B. Delley, From molecules to solids with the DMol³ approach, *J. Chem. Phys.* 113(18), 7756 (2000)
 33. A. Rubio-Ponce, A. Conde-Gallardo, and D. Olguin, First-principles study of anatase and rutile TiO₂ doped with Eu ions: A comparison of GGA and LDA + *U* calculations, *Phys. Rev. B* 78(3), 035107 (2008)
 34. A. Delin, L. Fast, B. Johansson, O. Eriksson, and J. M. Wills, Cohesive properties of the lanthanides: Effect of generalized gradient corrections and crystal structure, *Phys. Rev. B* 58(8), 4345 (1998)
 35. B. Delley, Hardness conserving semilocal pseudopotentials, *Phys. Rev. B* 66(15), 155125 (2002)
 36. S. L. Yue and H. Zhang, First principles study on magnetic and electronic properties with rare-earth atoms doped SWCNTs, *Front. Phys.* 7(3), 353 (2012)